Germ-layer commitment and axis formation in sea anemone embryonic cell aggregates

Anastasia Kirillova[a,b,1], Grigory Genikhovich[a,1,2], Ekaterina Pukhlyakova[a], Adrien Demilly[a], Yulia Kraus[b,c,2], and Ulrich Technau[a,2]

[a]Department for Molecular Evolution and Development, Center of Organismal Systems Biology, Faculty of Life Sciences, University of Vienna, A-1090 Vienna, Austria; [b]Department of Evolutionary Biology, Biological Faculty, Moscow State University, 119234 Moscow, Russia; and [c]Koltzov Institute of Developmental Biology, Russian Academy of Sciences, 119334 Moscow, Russia

Edited by Edward M. De Robertis, Howard Hughes Medical Institute and University of California, Los Angeles, CA, and approved January 5, 2018 (received for review June 27, 2017)

Robust morphogenetic events are pivotal for animal embryogenesis. However, comparison of the modes of development of different members of a phylum suggests that the spectrum of developmental trajectories accessible for a species might be far broader than can be concluded from the observation of normal development. Here, by using a combination of microsurgery and transgenic reporter gene expression, we show that, facing a new developmental context, the aggregates of dissociated embryonic cells of the sea anemone *Nematostella vectensis* take an alternative developmental trajectory. The self-organizing aggregates rely on Wnt signals produced by the cells of the original blastopore lip organizer to form body axes but employ morphogenetic events typical for normal development of distantly related cnidarians to re-establish the germ layers. The reaggregated cells show enormous plasticity including the capacity of the ectodermal cells to convert into endoderm. Our results suggest that new developmental trajectories may evolve relatively easily when highly plastic embryonic cells face new constraints.

self-organization | embryonic cell aggregates | body axes | germ layers

Animal embryonic development can be viewed as a robust series of morphogenetic events triggered and controlled by the action of regulatory molecules and physical characteristics of the cells and tissues. These morphogenetic events form a developmental trajectory enabling the formation of a certain body plan. Strikingly, the phylum-specific body plan can be reached by a variety of developmental trajectories. For example, among chordates, radial, holoblastic cleavage of the yolk-poor eggs of the cephalochordate *Branchiostoma* results in the formation of a hollow coeloblastula, which gastrulates by invagination. In contrast, discoidal cleavage of the bird egg results in the formation of a discoblastula lying on top of the yolk and gastrulating via ingression of single cells through the primitive streak (1). Regardless, both developmental trajectories lead to the formation of a typical chordate body plan. Similarly, among different cnidarians, virtually all known modes of gastrulation can be found (2). While invagination is predominant among anthozoans and scyphozoans, hydrozoans gastrulate by unipolar or multipolar ingression, delamination, or epiboly. Nevertheless, after gastrulation, all cnidarians (except a few direct developers) form a typical planula larva. How such differences in development evolved and how they may have contributed to the formation of different body plans remain open questions in biology.

A large body of experimental data indicates that the spectrum of potencies for differentiation and cell behavior in embryonic cells is broader than their prospective fate and actual behavior during normal development (3–7). An extreme case of developmental plasticity is observed in animals capable of developing from a clump of dissociated and reaggregated cells, when the initial body plan is destroyed and then re-established de novo by self-organization (8–11). We reasoned that new developmental trajectories might evolve when cells capable of regulative development respond to new physical constraints, such as the increasing amount of yolk in the abovementioned example. We hypothesized therefore that new developmental trajectories might also be used if embryonic cells face a new context in an experimental situation. To test the extent of the regulative capacity of embryonic cells, we performed dissociation–reaggregation experiments with embryos of the sea anemone *Nematostella vectensis*. In this study, we use a combination of microsurgery and transgenic reporter gene assays to assess the developmental potential of different embryonic cells originating from dissociated *Nematostella* gastrulae and analyze the process of reforming of the body axes and the germ layers.

Results and Discussion

Nematostella is a cnidarian model system amenable to functional studies in embryogenesis. Upon fertilization, the *Nematostella* embryo develops into a hollow blastula, which then gastrulates by invagination, forms a swimming planula larva, and metamorphoses into a primary polyp (12). Recent transplantation experiments have shown that the blastopore lip of the *Nematostella* gastrula has an axis-inducing capacity conveyed by *Wnt1* and *Wnt3*, similar to the blastoporal axial organizer of vertebrates (13, 14). To assess the developmental potential of different embryonic cells, we dissociated *Nematostella* midgastrulae, at the stage when the endoderm just starts to invaginate, into single cells or small clusters of

Significance

Embryonic development of any animal species is a robust series of morphogenetic events tightly controlled by molecular signals. However, the variety of developmental trajectories undertaken by different members of the same phylum suggests that normal development in each particular species might involve only a subset of morphogenetic capacities available to the highly developmentally plastic embryonic cells. Here we show that, faced by a new developmental context, the aggregates of dissociated gastrula cells of the sea anemone *Nematostella vectensis* use an alternative developmental trajectory typical for other, distantly related members of the cnidarian phylum. We conclude that new modes of development may evolve relatively easily due to the versatility and developmental plasticity of embryonic cells.

Author contributions: A.K., G.G., Y.K., and U.T. designed research; A.K., G.G., and E.P. performed research; E.P. and A.D. contributed new reagents/analytic tools; A.K. and G.G. analyzed data; and A.K., G.G., Y.K., and U.T. wrote the paper.

The authors declare no conflict of interest.

This article is a PNAS Direct Submission.

[1]A.K. and G.G. contributed equally to this work.

[2]To whom correspondence may be addressed. Email: grigory.genikhovich@univie.ac.at, yulia_kraus@hydrozoa.org, or ulrich.technau@univie.ac.at.

This article contains supporting information online at www.pnas.org/lookup/suppl/doi:10.1073/pnas.1711516115/-/DCSupplemental.

two to nine cells [~80 and ~20%, respectively (Fig. S1*A*)] and reaggregated them by centrifugation (Fig. 1*A*). Immediately after centrifugation, the aggregates lacked any sign of axial polarity or germ-layer segregation at both the morphological (Fig. 1 *B* and *C*) and the molecular (Fig. S2 *A*–*T*) level. The completeness of dissociation and the subsequent morphological observations were confirmed by in situ hybridization analysis of the oral markers *Wnt1*, *Wnt3*, *Wnt4*, *Bra*, and *FoxA*, midbody marker *Wnt2*, aboral marker *FGFa1*, endodermal marker *SnailA*, and directive axis markers *BMP2/4* and *Chordin* from 30 min post dissociation (mpd, i.e., immediately after reaggregation) until 6 d post dissociation (dpd) (Fig. S2). Ectodermal and endodermal cell layers began to segregate in several independent regions at 6–12 h post dissociation (hpd) (Fig. 1 *D* and *E*). The ectodermal cell layer formed first, while endoderm remained unepithelialized. By 24 hpd, the germ-layer segregation was complete (Fig. 1 *F* and *G*), and the endodermal marker *snailA* was expressed exclusively in the inner layer of the aggregates (Fig. S2*B*′). At the same stage, we observed the first signs of mouth formation (Fig. 1*H*). Starting from day 2 post dissociation, the aggregates were most similar to planulae: their ectoderm developed cilia, and the aggregates were actively swimming around. Interestingly, larger aggregates looked as if they were built of multiple fused planulae. Mouth and pharynx formation continued over the next 2 d (Fig. 1 *I*–*K*), and by day 6 the hypostomes (oral cones) had developed (Fig. 1*L*). Tentacle formation was complete by day 7–10 (Fig. 1*M*). Depending on the size of the aggregate, one or multiple oral openings formed. To monitor the formation of the oral–aboral axes in aggregates, we performed double in situ hybridization with the oral pole marker *FoxA* and the aboral pole marker *FGFa1* (15) (Fig. 1*N*). Interestingly, the number of *FoxA*-expressing spots exceeded the number of the *FGFa1*-expressing

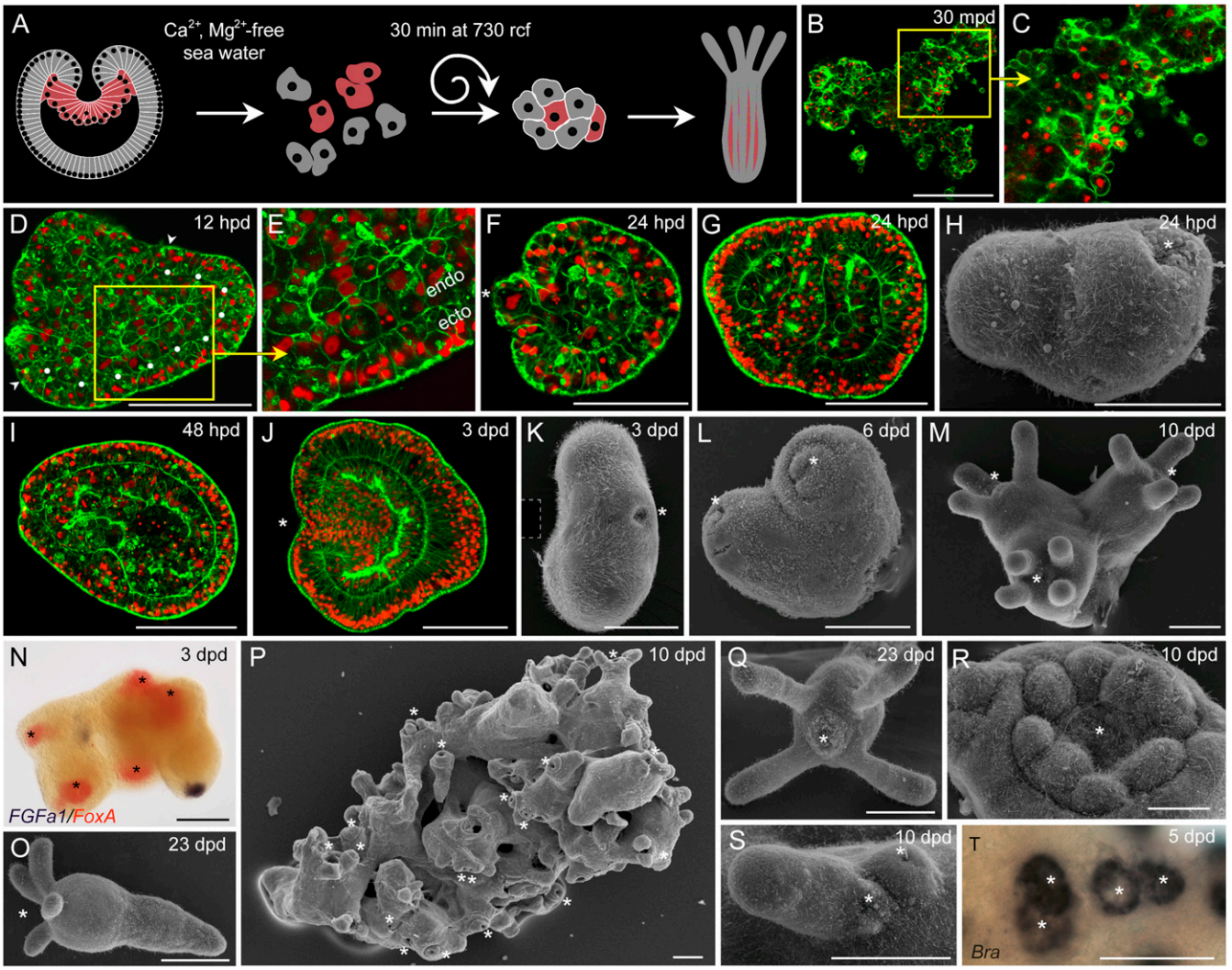

Fig. 1. The course of aggregate development. (*A*) Scheme of the dissociation–reaggregation experiment. (*B*–*M*) Successive stages of aggregate development analyzed by confocal and scanning electron microscopy. Directly after centrifugation, no epithelium is observed (*B* and *C*). Ectoderm epithelialization begins by 12 hpd (*D* and *E*: note a stretch of epithelialized ectoderm along the dotted line between white arrowheads in *D*) and is complete by 24 hpd (*F*: longitudinal optical section; *G*: transverse optical section). First signs of mouth formation become visible (*F* and *H*). Endoderm starts to form an epithelial layer by 48 hpd (*I*) and completes the process by 3 dpd (*J*: note also a well-developed pharynx). Mouth, hypostome, and tentacles form over the next several days (*K*–*M*). Black box (*K*, dashed line) masks the original scale bar. (*N*–*T*) Larger aggregates form multiple heads. (*N*) Double in situ hybridization with the oral marker *FoxA* (red) and aboral marker *FGFa1* (blue) shows that the number of heads/number of aboral poles ratio is 3/1. SEM shows that the number of heads per aggregate and tentacles per head can vary (*O*–*S*). Head structures can form in close proximity to each other, as visualized by SEM at the polyp stage and by in situ hybridization with an oral marker *Brachyury* at an earlier stage (*S* and *T*). (*B*–*G*, *I*, and *J*) Red: nuclei; green: F-actin. Asterisks, mouth; dpd, days post dissociation; ecto, ectoderm; endo, endoderm; hpd, hours post dissociation; mpd, minutes post dissociation. (Scale bars: 100 μm.)

spots by a factor of approximately 3 (mean: 2.98; 95% confidence interval: 2.69–3.27; median: 3.0; $n = 60$). Large aggregates always formed multiple heads with a varying number of tentacles (Fig. 1 *O–S*). Unlike in aggregates of the adult freshwater polyp *Hydra* (16), mouth openings were often located very close to each other (Fig. 1 *S* and *T*), indicating that lateral inhibition is not as prominent as in *Hydra*.

The experiments described above demonstrate that dissociated gastrula tissue of *Nematostella* is capable of re-establishing the normal body plan in the aggregates. Next, we wanted to know whether the self-organizing capacity was restricted to specific parts of the embryo. To this end, we generated aggregates from dissociated oral or aboral halves only. We found that the oral halves were capable of re-establishing the body axes, and eventually they developed into normal polyps (Fig. 2 *A–E*). In contrast, aboral aggregates formed ciliated balls without any sign of axial patterning containing a thin superficial epithelial layer and numerous small unepithelialized cells inside (Fig. 2 *F–J*). Recently, we showed that the capacity to induce ectopic body axes in transplantation experiments, i.e., the axial organizer capacity, is confined to a narrow area of the bend of the blastopore lip of the *Nematostella* gastrula (13). To estimate how many organizer cells are required to initiate axis formation in the aggregates, we determined the approximate amount of cells in the midgastrula at the time of dissociation (median: 6,934; Fig. S1*B*), and the number of cells in the single row of the bend of the blastopore lip (median: 107; Fig. S1*C*). Then we dissociated and reaggregated 100 aboral midgastrula halves together with 2, 5, or 10 oral gastrula halves, respectively, generating 1/50, 1/20, and 1/10 dilutions of oral gastrula halves by aboral gastrula halves. This corresponds to approximately 1/1,550, 1/620, and 1/310 ratios of the organizer cells to aboral half cells (in comparison with the 1/31 ratio when complete gastrulae are dissociated). We observed the formation of ciliated balls without any signs of body axes in all aggregates composed of 1 oral half per 50 aboral halves, 28% head formation in aggregates composed of 1 oral per 20 aboral halves, and 58% head formation in the aggregates composed of 1 oral per 10 aboral halves (Fig. S1*D*).

To find out whether aboral cells retain a memory of their original axial position after dissociation or adopt a new fate according to their new position, we generated a transgenic line ubiquitously expressing a fluorescent lifeact-mOrange2 actin-binding protein driven by an *EF1α* promoter (17–19) (Fig. S3 *A–C*). We then produced mixed aggregates from lifeact-mOrange2–expressing aboral gastrula halves with nontransgenic oral gastrula halves (Fig. 2*K*). We found that fluorescent cells dispersed throughout the entire resulting polyps, including their oral-most regions, indicating that the axial identity was reprogrammed in these originally aboral cells to adopt an oral identity (Figs. 2 *K–N* and 3).

Surprisingly, in this experiment, we detected some fluorescent transgenic cells inside the aggregates (Fig. S4 *A–D*), even though all transgenic lifeact-mOrange2 cells originated from aboral gastrula halves, i.e., prospective ectoderm. We therefore wanted to test more rigorously whether the cells in the aggregate kept their original germ-layer identity. In this respect, two scenarios could be envisaged: (*i*) either the embryonic cells sort out in accordance to their original germ-layer identity as shown in amphibians (20) or (*ii*) they lose the information about their initial germ-layer identity and acquire it de novo in the course of aggregate development. We dissected fluorescent pre-endodermal plates out of the lifeact-mOrange2 embryos using microsurgical techniques (Fig. 2*O*). Then we dissociated these fragments together with the nontransgenic ectodermal cells. We observed that during the first 18 h of aggregate development all fluorescently labeled cells migrated into the inside of the aggregate (Fig. 2 *O–R* and Movie S1). Therefore, we conclude that endodermal cells "remember" their initial fate and are able to sort out to form the inner layer of an aggregate (Fig. 3). Interestingly, the signal necessary for the individual ingression of the endodermal cells does not emanate from the organizer cells of the blastopore lip, since ingression of the endodermal cells also happened in the aggregates made of *EF1a::lifeact-mOrange2* endoderm and aboral ectoderm of the wild-type gastrulae (Fig. 2 *S–V*). Similarly to the aboral half-aggregates (Fig. 2 *G–J*), such aggregates developed into compact balls with an ectodermal layer and a mass of cells inside (Fig. 2 *S–V*). To test whether endodermal cells alone would be able to form aggregates and develop into polyps, we made aggregates out of surgically isolated pre-endodermal plates (Fig. 2*W*). Strikingly, without an ectoderm forming an epithelium on the surface of the aggregate, the endodermal cells became mesenchymal and dispersed. At 3.5 hpd, cells forming filopodia could be observed at the edge of the aggregate. By 12 hpd, the whole aggregate converted to viable, motile mesenchymal cells spread on the surface of the dish, failing to develop and form a polyp (Fig. 2 *W–Z*). Thus, endoderm alone is unable to compensate for the absence of ectoderm.

We then carried out the reciprocal experiment, i.e., forming aggregates consisting of only ectodermal cells. If ectodermal cells are capable of converting into endoderm, we expect them to be located in the inner layer, and—importantly—to start expressing endoderm-specific marker genes. To monitor this conversion, we generated a transgenic line called endoRed, expressing mCherry exclusively in the endoderm under control of the regulatory region of the *SnailA* gene, which encodes an endodermally expressed zinc-finger transcription factor (Fig. S3 *D–F*) (21). By microsurgery, we isolated aboral halves of endoRed offspring gastrulae containing only ectodermal cells. Since aggregates from aboral hemispheres fail to develop into primary polyps (Fig. 2 *F–J*), we dissociated them together with the blastopore lip fragments of the wild-type gastrulae (Fig. 2*A′*). We excluded the possibility of contamination of the aboral halves of the endoRed offspring embryos with the mCherry-expressing cells of the pre-endodermal plate (Fig. 2*B′*; see *SI Materials and Methods* for details) and then followed the development of the aboral endoRed/wild-type blastopore lip aggregates, where not a single fluorescent cell was detected after reaggregation. Thus, any mCherry-expressing cells appearing as the aggregates develop must have originated from aboral ectoderm of the endoRed line. After 1 d, we detected the first cells expressing the endoderm-specific transgene inside the aggregates (Fig. 2*C′*). These cells persisted throughout development, and eventually primary polyps formed with fluorescent patches in the endoderm (Fig. 2 *D′* and *E′*). By comparison, control aggregates made of oral halves of the endoRed gastrulae were fluorescent from the start (Fig. 2 *F′–J′*). Therefore, we conclude that the ectodermal cells of the endoRed embryos were able to contribute to the endoderm of the polyp (Fig. 3). To test whether the presence of wild-type endodermal cells would prevent aboral ectoderm cells from adopting an endodermal fate, we dissociated aboral halves of the endoRed gastrulae together with whole oral halves of wild-type gastrulae including nontransgenic endodermal cells. Notably, we found that the presence of the nontransgenic endoderm did not prevent some aboral ectodermal endoRed cells located inside these aggregates from adopting an endodermal fate (Fig. S4 *E–H*). Interestingly, even in the absence of oral cells, single mCherry-expressing cells were transiently detectable in the aboral ectodermal aggregates, yet this expression faded as the aggregates were arrested in the ciliated ball stage (Fig. S4 *I–L*). This suggests that the internal location might be sufficient to initiate the expression of endodermal marker genes in the aboral ectodermal cells, yet this expression needs to be maintained by signals coming from the blastopore lip cells.

The above result raises the question, which signals emanating from the blastoporal cells could induce and maintain axis and germ-layer formation? Since endodermal cells were capable of sorting out autonomously in the absence of axis-forming signals (Fig. 2 *S–V*), we reasoned that axis formation is central for the development of the aggregates. Therefore, we focused on the role of Wnt/β-catenin signaling and BMP signaling as the signaling

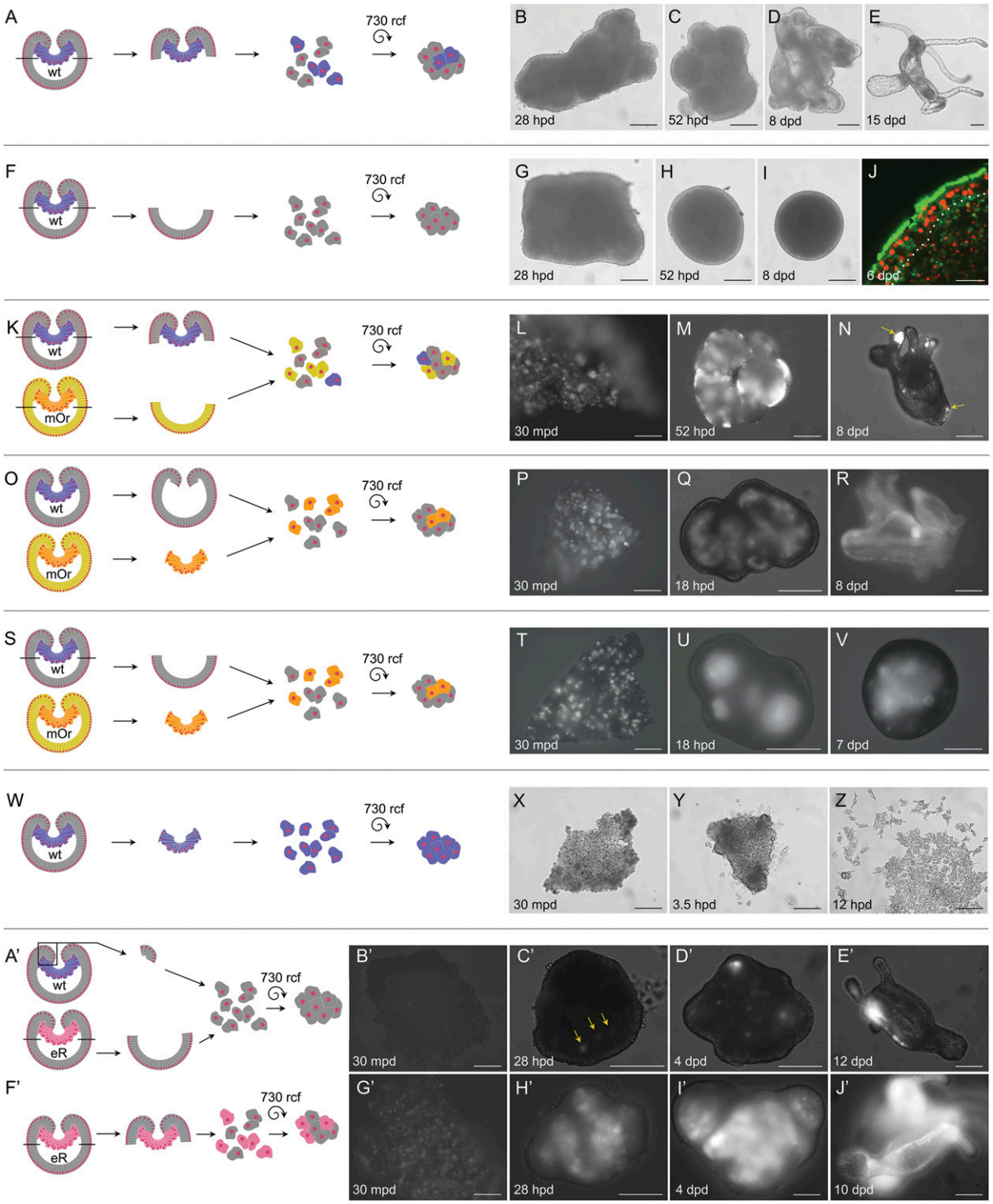

Fig. 2. Differences in capacities of gastrula cells for axis formation and cell-fate specification in the aggregates. (*A–E*) Aggregates made of oral halves of gastrulae develop into polyps. (*F–J*) Aggregates made of aboral halves of gastrulae develop into ciliated balls. (*J*) Confocal imaging shows that, outside, they have an ectodermal epithelial layer and that their inside is filled with numerous small cells. (*K–N*) In aggregates made of oral halves of wild-type gastrulae and aboral halves of gastrulae ubiquitously expressing lifeact-mOrange2, glowing cells are dispersed throughout the aggregate and can be observed both in aboral and oral positions of the polyp (yellow arrows in *N*). (*O–R*) In aggregates made of ectoderm of wild-type gastrulae and endoderm of gastrulae ubiquitously expressing lifeact-mOrange2, fluorescent cells migrate into the endoderm. (*S–V*) In aggregates made of aboral ectoderm of wild-type gastrulae and endoderm of gastrulae ubiquitously expressing lifeact-mOrange2, fluorescent cells migrate into the endoderm although the organizer cells are missing. (*W–Z*) In aggregates made of only endodermal cells, the cells become mesenchymal and migrate out of the aggregate. (*A′–E′*) Immediately after centrifugation, mCherry is not expressed in aggregates made of aboral ectoderm of endoRed gastrulae and blastopore lip ectoderm of the wild-type gastrulae (*B′*). Endodermal promoter-driven mCherry expression starts to be detectable in the internal cells of the aggregate from 28 hpd on (yellow arrows in *C′*). Glowing cells are then observed in the endoderm of the forming polyps (*E′*). (*F′–J′*) In aggregates made of oral halves of endoRed gastrulae, mCherry is continuously expressed in the endodermal cells. Sample size >30 in every experiment. dpd, days post dissociation; eR, endoRed; hpd, hours post dissociation; mOr, lifeact-mOrange2; mpd, minutes post dissociation; wt, wild type. Black bars on gastrulae denote the position of the cut. (Scale bars: *J*, 15 μm; all others, 100 μm.)

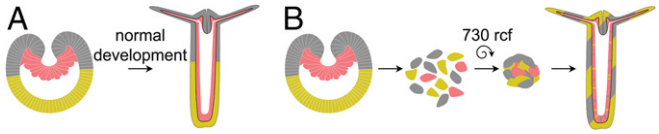

Fig. 3. The summary of the fate of cells during normal development (*A*) and in aggregates (*B*).

molecules of these pathways are expressed at the blastopore and they have previously been shown to have a role in axis formation in *Nematostella* (13, 22–26).

β-catenin knockdown results in the lack of an oral–aboral axis and endoderm formation (22, 23). During normal development, the initial β-catenin signal is most likely based on maternally deposited molecules (13, 27), while the zygotic expression of *Wnt* genes starts to be detectable by in situ hybridization at some point between 6 and 10 hpf (13). Recent transplantation experiments demonstrated that *Wnt1* and *Wnt3* expressed in the blastopore lip are sufficient to convey axial organizer capacity to aboral ectodermal cells of the *Nematostella* gastrula (13). To test whether these two signaling molecules are required for proper axial development and endoderm formation in aggregates, we injected random single blastomeres at the eight-cell stage with plasmids driving the expression of *Wnt1* and *Wnt3* and then made aggregates out of the aboral halves of these injected embryos when they reached the midgastrula stage. Although lacking the pre-endodermal plate cells and the blastopore lip cells, these aggregates developed into primary polyps (Fig. 4 *A–C*). This indicates that *Wnt1* and *Wnt3* are sufficient to rescue proper germ-layer and axis formation and induce self-organization of embryonic aggregates.

BMP signaling plays the central role in establishing and maintaining the second, directive body axis in *Nematostella* (24–26). During normal development, the initial, radially symmetric expression of the central BMP-signaling components *BMP2/4* and *Chordin* starts to be detectable in the blastula around 14 hpf (13) in a β-catenin–dependent manner (Fig. S5*A*). At late gastrula, a BMP-signaling–dependent symmetry break in the expression of *BMP2/4* and *Chordin* occurs, manifesting the establishment of the directive axis (28). Consequently, morpholino knockdown of *BMP2/4* or *Chordin* results in the loss of BMP signaling in the embryo and the lack of the directive axis (24, 25). To assess the role of BMP signaling in self-organizing aggregates, we made aggregates from gastrula-stage embryos injected with the previously tested BMP2/4 morpholino (24). Strikingly, BMP2/4MO aggregates were not only unable to form the directive axes, as we would expect, but also their oral–aboral axes were strongly affected (Fig. 4 *D–F*). Morpholino knockdown of BMP ligands has already been shown to influence the expression of many genes transcribed in restricted domains along the oral–aboral axis (24, 26, 29), suggestive of a possible feedback of the BMP signaling onto the Wnt/β-catenin–signaling system. We set out to test this in more detail in BMP2/4 morphants and morphant aggregates. Although the expression of the inducers of oral development, *Wnt1* and *Wnt3*, was up-regulated in the 24-hpf BMP2/4 morphant gastrula transcriptome (29), *Wnt1*, *Wnt3*, *FoxA*, and *Brachyury* expression domains appeared normal in the BMP2/4 morphants at the 24-hpf gastrula stage. In contrast, the expression of all these genes appeared significantly weaker in 2- and 3-d-old morphant embryos (Fig. S5*B*). Similarly, the expression of *Wnt1*, *Wnt3*, and *Brachyury* was also reduced, and its restriction to the oral poles was severely affected in the BMP2/4MO aggregates (Fig. S6*A*). If BMP signaling is required for the maintenance of the proper expression of *Wnt1* and *Wnt3*, its down-regulation should suppress the inductive capacity of the blastopore lip organizer cells. In line with that, we observed a strong reduction of the axis-inducing capacity of the blastopore lips transplanted from *BMP2/4* and *Chordin* morphant donors to the wild-type recipients (Fig. S5*C*). The presence of the positive feedback of BMP signaling on Wnt/β-catenin signaling also explains our previous observation that, unlike in vertebrates, single-blastomere injection of *Chordin* expression constructs does not lead to the formation of ectopic body axes in *Nematostella*. Paradoxically, analysis of *Frizzled 5/8* expression in BMP2/4 morphants and morphant aggregates suggests that the reduction of the expression of the oral markers *Wnt1*, *Wnt3*, *FoxA*, and *Brachyury* is not accompanied by the expansion of the aboral territory characterized by low levels of β-catenin signaling, but rather by a reduction in *Fz5/8* expression in older morphants and BMP2/4MO aggregates (Figs. S5*B* and S6*B*).

Our experiments showed that aggregates of embryonic cells of the sea anemone *Nematostella* are capable of re-establishing the germ layers and correct axial patterning of the body. Endodermal cells in the aggregates maintained their endodermal identity and were unable to convert into ectoderm, suggesting that this early cell-fate decision is irreversible. Moreover, endodermal cells were able to ingress from the surface of the aggregate autonomously, i.e., in the absence of the oral cells. However, such aggregates remained solid spheres, which suggests that oral signals might still be required for the formation of the defined endodermal layer. Aggregates made exclusively of endodermal cells did not reform polyps but converted into mesenchymal cells. By contrast, ectodermal cells were capable of converting into endoderm and forming normal polyps. Axial patterning in the aggregates relied on Wnt signals from the blastopore lip ectoderm, which has organizer activity (13–15). In contrast, the cells originating from aboral ectoderm acquired new axial identity once dispersed throughout the aggregate. Our results also highlight the importance of BMP signaling in the maintenance of the Wnt-dependent oral–aboral axis in *Nematostella*.

Since the aggregates utilize the same set of developmental regulators as normal embryos, we conclude that these genes are part of a self-organizing gene regulatory network enabling stunning plasticity and ability to respond to a yet-unprecedented developmental context, such as the lack of the cavity in the aggregate, which prevents invagination. To circumvent this constraint, the aggregates of the sea anemone *Nematostella* activate an alternative

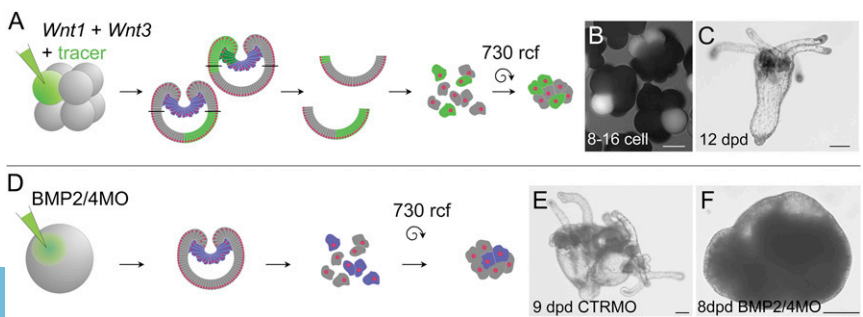

Fig. 4. The role of Wnt/β-catenin and BMP signaling during aggregate development. (*A–C*) Axis formation and endoderm segregation is rescued in 15 of 17 aggregates made from aboral halves of gastrulae, which were coinjected into a single blastomere at the eight-cell stage with plasmids coding for untagged Wnt1 and Wnt3 driven by the *EF1α* promoter and fluorescent tracer (glowing cells in *B*). (*D–F*) *BMP2/4* knockdown results in the lack of morphologically distinct body axes in the aggregates. $n = 32$. (Scale bars: 100 μm.)

developmental trajectory. Instead of invagination, they form germ layers by a combination of delamination of the ectodermal layer; multipolar ingression of the endodermal plate cells, which happened to end up on the surface of the aggregates after centrifugation of the dissociated cells; and cavitation of the mass of cells located inside the aggregates. Curiously, the experimentally modulated development in *Nematostella* aggregates resembles the normal development of other cnidarians, i.e., members of Hydrozoa, which gastrulate usually by ingression of individual cells (30, 31) or delamination (32, 33) (Fig. S7*A*). Unlike gastrulation in most cnidarians and in Bilateria, where it occurs at a certain position in relation to the body axes of an embryo, delamination and ingression in Hydrozoa can be multipolar and not linked to the axial patterning (32–37) (Fig. S7*A*). During morula delamination, when a solid embryo without a blastocoel forms as a result of cleavage, external cells of a morula start to epithelialize and segregate themselves from the inner mass of cells, the future endoderm, which then cavitates and forms an endodermal epithelial layer. In resemblance to the situation during *Nematostella* aggregate development (Fig. S7 *B*–*E*), the epithelialization of the ectoderm starts in many different regions throughout the morula, and then individual patches of epithelium expand and fuse (32, 33).

Such plasticity is not a unique feature of the embryonic cells of early branching metazoans. In sea urchins and sea stars, dissociated and reaggregated cells of gastrula-stage embryos are just as capable of re-establishing their normal body plans and forming larvae. Interestingly, also in echinoderms, the inner cells of the aggregates form the endodermal layer omitting the invagination step (38–41). However, once the inner cells arrange into an epithelium, and the embryo cavitates, the coelomic pouches form by an enterocoelic process (42), i.e., from evaginations of the gut wall. The comparison of aggregates and normal embryos suggests that alternative developmental trajectories are easily accessible to organisms, unless they have highly derived mosaic development. Moreover, it is likely that this kind of plasticity and the capacity for regulative development were present already at the earliest stages of animal evolution. Since phenotype robustness promotes phenotype evolvability (43), the capacity to change embryonic development without deleterious effects might have facilitated the diversification of the developmental trajectories leading to the formation of animal body plans.

Materials and Methods

Details on the animal culture, transgenic lines, embryo manipulations, microinjections, analyses of dissociation efficiency and determination of the number of the cells in the bend of the blastopore lip, as well as the molecular and histological techniques can be found in the *SI Materials and Methods*.

ACKNOWLEDGMENTS. S. Lysenkov assisted with the statistical analysis; SEM was performed at the Electron Microscopy Laboratory of the Shared Facilities Center of the Moscow State University; and confocal imaging was performed at the Core Facility for Cell Imaging and Ultrastructure Research of the University of Vienna. This work was funded by Austrian Science Foundation Grants P22717 (to U.T.) and P26962 (to G.G.) and by federal project 0108-2018-0003 of the Koltzov Institute of Developmental Biology of the Russian Academy of Sciences (to Y.K.). A.K. was a recipient of a European Molecular Biology Organization short-term fellowship (ASTF 357–2015) and of an Austrian Academic Exchange Service stipend (ICM-2013-03977).

1. Gilbert SF, Raunio AM, eds (1997) *Embryology: Constructing the Organism* (Sinauer Associates, Sunderland, MA), p 538.
2. Tardent P, ed (1978) *Coelenterata, Cnidaria* (Gustav Fischer, Stuttgart).
3. Morgan TH (1895) Half embryos and whole embryos from one of the first two blastomeres. *Anat Anz* 10:623–638.
4. Driesch H (1891) Entwicklungsmechanische Studien I, II [Studies on developmental mechanics I, II]. *Z Wiss Zool* 53:160–184. German.
5. Hörstadius S (1939) The mechanics of sea urchin development. *Biol Rev Camb Philos Soc* 14:132–179.
6. Takahashi K, Yamanaka S (2015) A developmental framework for induced pluripotency. *Development* 142:3274–3285.
7. Green JB, Dominguez I, Davidson LA (2004) Self-organization of vertebrate mesoderm based on simple boundary conditions. *Dev Dyn* 231:576–581.
8. Wilson HV (1907) On some phenomena of coalescence and regeneration in sponges. *J Exp Zool* 5:245–258.
9. Wilson HV (1911) On the behavior of the dissociated cells in hydroids, alcyonaria, and Asterias. *J Exp Zool* 11:281–338.
10. Gierer A, et al. (1972) Regeneration of hydra from reaggregated cells. *Nat New Biol* 239:98–101.
11. Nieuwkoop PD (1992) The formation of the mesoderm in urodelean amphibians VI. The self-organizing capacity of the induced meso-endoderm. *Rouxs Arch Dev Biol* 201:18–29.
12. Genikhovich G, Technau U (2009) The starlet sea anemone *Nematostella vectensis*: An anthozoan model organism for studies in comparative genomics and functional evolutionary developmental biology. *Cold Spring Harb Protoc* 2009:pdb.emo129.
13. Kraus Y, Aman A, Technau U, Genikhovich G (2016) Pre-bilaterian origin of the blastoporal axial organizer. *Nat Commun* 7:11694.
14. Kraus Y, Fritzenwanker JH, Genikhovich G, Technau U (2007) The blastoporal organiser of a sea anemone. *Curr Biol* 17:R874–R876.
15. Fritzenwanker JH, Genikhovich G, Kraus Y, Technau U (2007) Early development and axis specification in the sea anemone Nematostella vectensis. *Dev Biol* 310:264–279.
16. Technau U, et al. (2000) Parameters of self-organization in *Hydra* aggregates. *Proc Natl Acad Sci USA* 97:12127–12131.
17. Riedl J, et al. (2008) Lifeact: A versatile marker to visualize F-actin. *Nat Methods* 5: 605–607.
18. Shaner NC, et al. (2008) Improving the photostability of bright monomeric orange and red fluorescent proteins. *Nat Methods* 5:545–551.
19. Steinmetz PRH, Aman A, Kraus JEM, Technau U (2017) Gut-like ectodermal tissue in a sea anemone challenges germ layer homology. *Nat Ecol Evol* 1:1535–1542.
20. Townes PL, Holtfreter J (1955) Directed movements and selective adhesion of embryonic amphibian cells. *J Exp Zool* 128:53–120.
21. Martindale MQ, Pang K, Finnerty JR (2004) Investigating the origins of triploblasty: 'Mesodermal' gene expression in a diploblastic animal, the sea anemone Nematostella vectensis (phylum, Cnidaria; class, Anthozoa). *Development* 131:2463–2474.
22. Wikramanayake AH, et al. (2003) An ancient role for nuclear beta-catenin in the evolution of axial polarity and germ layer segregation. *Nature* 426:446–450.
23. Leclère L, Bause M, Sinigaglia C, Steger J, Rentzsch F (2016) Development of the aboral domain in Nematostella requires β-catenin and the opposing activities of six3/6 and frizzled5/8. *Development* 143:1766–1777.
24. Saina M, Genikhovich G, Renfer E, Technau U (2009) BMPs and chordin regulate patterning of the directive axis in a sea anemone. *Proc Natl Acad Sci USA* 106:18592–18597.
25. Genikhovich G, et al. (2015) Axis patterning by BMPs: Cnidarian network reveals evolutionary constraints. *Cell Rep* 10:1646–1654.
26. Leclère L, Rentzsch F (2014) RGM regulates BMP-mediated secondary axis formation in the sea anemone Nematostella vectensis. *Cell Rep* 9:1921–1930.
27. Lee PN, Kumburegama S, Marlow HQ, Martindale MQ, Wikramanayake AH (2007) Asymmetric developmental potential along the animal-vegetal axis in the anthozoan cnidarian, Nematostella vectensis, is mediated by dishevelled. *Dev Biol* 310:169–186.
28. Rentzsch F, et al. (2006) Asymmetric expression of the BMP antagonists chordin and gremlin in the sea anemone Nematostella vectensis: Implications for the evolution of axial patterning. *Dev Biol* 296:375–387.
29. Wijesena N, Simmons DK, Martindale MQ (2017) Antagonistic BMP-cWNT signaling in the cnidarian Nematostella vectensis reveals insight into the evolution of mesoderm. *Proc Natl Acad Sci USA* 114:E5608–E5615.
30. Momose T, Schmid V (2006) Animal pole determinants define oral-aboral axis polarity and endodermal cell-fate in hydrozoan jellyfish Podocoryne carnea. *Dev Biol* 292:371–380.
31. Byrum CA (2001) An analysis of hydrozoan gastrulation by unipolar ingression. *Dev Biol* 240:627–640.
32. Kraus YA (2006) Morphomechanical programming of morphogenesis in cnidarian embryos. *Int J Dev Biol* 50:267–275.
33. Kraus Y, et al. (2014) The embryonic development of the cnidarian Hydractinia echinata. *Evol Dev* 16:323–338.
34. Allman GJ (1871) *A Monograph on the Gymnoblastic or Tubularian Hydroids. Vol. I: The Hydroida in General* (Forgotten Books, London), p 154.
35. Schulze FE (1871) *Über den Bau und die Entwicklung von Cordylophora lacustris (Allman)* [*On the anatomy and the development of Cordylophora lacustris (Allman)*] (Wilhelm Engelmann, Leipzig, Germany), p 55. German.
36. Metschnikoff E (1874) Studien über die Entwicklung der Medusen und Siphonophoren. (Studies of the development of jellyfish and siphonophores) *Z Wiss Zool* 24:15–80. German.
37. Harm K (1903) Die Entwicklung von Clava squamata [The development of Clava squamata]. *Z Wiss Zool* 73:115–165. German.
38. Dan-Sohkawa M, Yamanaka H, Watanabe K (1986) Reconstruction of bipinnaria larvae from dissociated embryonic cells of the starfish, Asterina pectinifera. *J Embryol Exp Morphol* 94:47–60.
39. Giudice G (1962) Restitution of whole larvae from disaggregated cells of sea urchin embryos. *Dev Biol* 5:402–411.
40. Yamanaka H, Tanaka-Ohmura Y, Dan-Sohkawa M (1986) What do dissociated embryonic cells of the starfish, Asterina pectinifera, do to reconstruct bipinnaria larvae? *J Embryol Exp Morphol* 94:61–71.
41. Spiegel M, Spiegel ES (1975) The reaggregation of dissociated embryonic sea-urchin cells. *Am Zool* 15:583–606.
42. Tamura M, Dan-Sohkawa M, Kaneko H (1998) Coelomic pouch formation in reconstructing embryos of the starfish Asterina pectinifera. *Dev Growth Differ* 40:567–575.
43. Wagner A (2008) Robustness and evolvability: A paradox resolved. *Proc Biol Sci* 275: 91–100.